Kinetics and Mechanism of the Reactions of 2,3-Butadione with F and Cl Atoms, UV Absorption Spectra of $CH_3C(O)C(O)CH_2\cdot$ and $CH_3C(O)C(O)CH_2O_2\cdot$ Radicals, and Atmospheric Fate of $CH_3C(O)C(O)CH_2O\cdot$ Radicals

L. K. Christensen, J. Sehested,[†] and O. J. Nielsen*[,‡]

Atmospheric Chemistry, Plant Biology and Biogeochemistry Department, Risø National Laboratory, DK-4000 Roskilde, Denmark

T. J. Wallington,*[,§] A. Guschin,[||] and M. D. Hurley

Ford Research Laboratory, SRL-3083, Ford Motor Company, Dearborn, P.O. Box 2053, Michigan 48121-2053

Received: June 1, 1998; In Final Form: August 12, 1998

FTIR-smog chamber techniques were used to determine rate constants for the gas-phase reaction of Cl and F atoms with $CH_3C(O)C(O)CH_3$ and F atoms with $CH_3C(O)F$ of $(4.0 \pm 0.5) \times 10^{-13}$, $(4.9 \pm 0.7) \times 10^{-11}$, and $(3.6 \pm 0.4) \times 10^{-12}$ cm^3 molecule^{-1} s^{-1}, respectively. Two pathways for the reaction of Cl and F atoms with $CH_3C(O)C(O)CH_3$ were found: (1a) $Cl + CH_3C(O)C(O)CH_3 \rightarrow HCl + CH_3C(O)C(O)CH_2\cdot$, (1b) $Cl + CH_3C(O)C(O)CH_3 \rightarrow CH_3C(O)Cl + CH_3C(O)\cdot$, (2a) $F + CH_3C(O)C(O)CH_3 \rightarrow HF + CH_3C(O)C(O)CH_2\cdot$, (2b) $F + CH_3C(O)C(O)CH_3 \rightarrow CH_3C(O)F + CH_3C(O)\cdot$, with branching ratios of $k_{1b}/(k_{1b} + k_{1a}) = 0.23 \pm 0.02$ and $k_{2b}/(k_{2b} + k_{2a}) = 0.56 \pm 0.09$. It was determined that the atmospheric fate of $CH_3C(O)C(O)CH_2O\cdot$ radicals is decomposition to give HCHO, CO, and $CH_3C(O)\cdot$ radicals. Pulse radiolysis coupled to UV absorption spectroscopy was used to study the kinetics of the reaction of F atoms with $CH_3C(O)C(O)CH_3$ as well as spectra of $CH_3C(O)C(O)CH_2\cdot$ and $CH_3C(O)C(O)CH_2O_2\cdot$ radicals over the wavelength range 220−400 nm at 295 K. The rate constant for the reaction of F atoms with $CH_3C(O)C(O)CH_3$ was determined to be $(4.6 \pm 0.8) \times 10^{-11}$ cm^3 molecule^{-1} s^{-1}. The absorption cross sections of $CH_3C(O)C(O)CH_2\cdot$ and $CH_3C(O)C(O)CH_2O_2\cdot$ radicals were $(5.4 \pm 1.0) \times 10^{-18}$ at 250 nm and $(2.0 \pm 0.5) \times 10^{-18}$ cm^2 molecule^{-1} at 320 nm, respectively. Results are discussed with respect to the available database concerning the reaction of Cl and F atoms with organic compounds.

1. Introduction

Dicarbonyl compounds are formed in the atmosphere by photooxidation of aromatic hydrocarbons. 2,3-Butadione is an oxidation product of *o*-xylene.[1−3] Atkinson et al.[1] reported a 2,3-butadione yield of 0.137 ± 0.016, and Darnall[3] a yield of 0.18 ± 0.04, both at atmospheric pressure in the presence of NO. The content of *o*-xylene in fuels can be substantial (up to 3.3 wt %[4]). Studies of the chemical composition of vehicle exhaust gas[5,6] show that the average emission of *o*-xylene from a Ford Taurus is of the order of 2−5 mg/m. Plum et al.[7] showed that photolysis is the major loss process of 2,3-butadione in the troposphere. The present study of 2,3-butadione concerns chemistry which is useful in the design and interpretation of laboratory studies, where F or Cl atoms are used to generate alkyl radicals. We show here that the reaction of 2,3-butadione with Cl and F atoms proceeds via two channels:

$$Cl + CH_3C(O)C(O)CH_3 \rightarrow HCl + CH_3C(O)C(O)CH_2\cdot \quad (1a)$$

$$Cl + CH_3C(O)C(O)CH_3 \rightarrow CH_3C(O)Cl + CH_3C(O)\cdot \quad (1b)$$

$$F + CH_3C(O)C(O)CH_3 \rightarrow HF + CH_3C(O)C(O)CH_2\cdot \quad (2a)$$

$$F + CH_3C(O)C(O)CH_3 \rightarrow CH_3C(O)F + CH_3C(O)\cdot \quad (2b)$$

Displacement reactions such as those shown in channels 1b and 2b could be important in the reaction of Cl and F atoms with other carbonyl compounds.

2. Experimental Section

The two experimental systems used have been described previously,[8,9] and are described briefly here.

2.1 FTIR−Smog Chamber System at Ford Motor Company. Experiments were performed using a 140 L Pyrex reactor interfaced to a Mattson Sirus 100 FTIR spectrometer.[8] The reactor was surrounded by 22 fluorescent blacklamps (GE F15T8-BL) which were used to photochemically initiate the experiments. The oxidation of 2,3-butadione was initiated by reaction with Cl or F atoms generated by the photolysis of molecular chlorine or fluorine in O_2/N_2 diluent at 700 Torr total pressure at 295 ± 2 K

* Authors to whom correspondence should be addressed.
[†] Present address: Haldor Topsø A/S, Nymøllevej 55, DK-2800 Lyngby, Denmark.
[‡] E-mail: ole-john.nielsen@riso.dk.
[§] E-mail: twalling@ford.com.
[||] Present address: Department of Earth, Atmospheric and Planetary Sciences, Massachusetts Institute of Technology, Cambridge, MA 02139.

10.1021/jp982431y CCC: $15.00
Published on Web 10/16/1998

$$Cl_2 \text{ (or } F_2) + h\nu \rightarrow 2 \text{ Cl (or 2 F)} \quad (3)$$

The loss of 2,3-butadione and formation of products were monitored by Fourier transform infrared spectroscopy using an infrared path length of 27 m and a resolution of 0.25 cm^{-1}. Infrared spectra were derived from 32 co-added interferograms.

Three sets of experiments were performed. First, a relative rate technique was used to determine the rate constants for reactions of Cl and F atoms with 2,3-butadione. Second, the mechanisms of Cl and F atom reactions with 2,3-butadione were investigated. Third, information concerning the atmospheric fate of $CH_3C(O)C(O)CH_2O\cdot$ radicals was gathered by irradiating $CH_3C(O)C(O)CH_3/NO/Cl_2/O_2/N_2$ mixtures.

2.2 Pulse Radiolysis System. A pulse radiolysis transient UV absorption apparatus was used to study the kinetics of reaction 2 as well as the UV absorption spectra of $CH_3C(O)C(O)CH_2\cdot$ and $CH_3C(O)C(O)CH_2O_2\cdot$ radicals. Radicals were generated by radiolysis of gas mixtures in a 1 L stainless steel reactor using a 30 ns pulse of 2 MeV electrons from a Febetron 705B field emission accelerator. The radiolysis dose, referred to herein as a fraction of maximum dose, was varied by insertion of stainless steel attenuators between the accelerator and the chemical reactor. The analyzing light was obtained from a pulsed xenon arc lamp and reflected in the reaction cell by internal White-type optics. The length of the cell is 10 cm and the optical path length for the analysis light was 120 cm. The analyzing light was monitored by a 1 m McPherson monochromator linked to a Hamamatsu R928 photomultiplier and a LeCroy 9450A oscilloscope. The monochromator was operated at a spectral resolution of 0.8 nm. UV absorption spectra were measured using a Princeton Applied Research OMA-II diode array installed at the exit slit of the monochromator in place of the photomultiplier. The monochromator was operated at a spectral resolution of 0.8 nm when used with the diode array. Spectral calibration was achieved using a Hg pen ray lamp. UV absorption spectra in the range 220−400 nm were acquired using the diode array with a radiolysis dose which was 53% of the maximum and a data acquisition time of 0.6−4.6 μs. The spectra given here are averages of three individual measurements.

All transients were results of single pulse experiments with no signal averaging. Data acquisition, handling, and storage were performed by a standard PC. The uncertainties reported in this paper are two standard deviations. Standard error propagation methods are used to calculate combined uncertainties.

SF_6 was used as diluent gas in the stainless steel reactor. Radiolysis of SF_6 produces fluorine atoms:

$$SF_6 \xrightarrow{\text{MeV e}^-} F + \text{products} \quad (4)$$

SF_6 was always in great excess to minimize the relative importance of direct radiolysis of other compounds in the gas mixtures. The direct radiolysis of 2,3-butadione is given approximately by its mass fraction. For the concentrations given in this work, direct radiolysis accounts for less than 0.3% of the 2,3-butadione loss. The fluorine atom yield was determined by measuring the yield of $CH_3O_2\cdot$ radicals following radiolysis of mixtures of 10 mbar of CH_4, 40 mbar of O_2, and 950 mbar of SF_6

$$F + CH_4 \rightarrow CH_3\cdot + HF \quad (5)$$

$$CH_3\cdot + O_2 + M \rightarrow CH_3O_2\cdot + M \quad (6)$$

The absorption of $CH_3O_2\cdot$ radicals at 260 nm was monitored as a function of radiolysis dose. In the presence of excess O_2 the $CH_3\cdot$ radical self-reaction is negligible and the $CH_3O_2\cdot$ yield equals the initial F atom yield. Using $\sigma(CH_3O_2\cdot) = (3.18 \pm 0.32) \times 10^{-18}$ cm^2 $molecule^{-1}$ [10] at 260 nm, the F atom yield was determined to be $(2.98 \pm 0.34) \times 10^{15}$ cm^{-3} at full radiolysis dose and 1000 mbar of SF_6. The quoted uncertainty reflects both statistical uncertainty in the measured absorbencies of $CH_3O_2\cdot$ and a 10% uncertainty in $\sigma(CH_3O_2\cdot)$.

Reagents used were the following: 0−27 mbar of O_2 (ultrahigh purity), 950−1000 mbar of SF_6 (99.9%), 0−19 mbar of $CH_3C(O)C(O)CH_3$ (>97%), 0−0.95 of mbar NO (>99.8%), 0−1.3 mbar of NO_2 (>98%), and 0−10 mbar of CH_4 (>99%). The $CH_3C(O)C(O)CH_3$ was repeatedly degassed by freeze−pump−thaw cycling before use. All other reagents were used as received.

Three sets of experiments were performed. First, the rate constant for reaction of F atoms with 2,3-butadione was measured. Second, the formation of alkyl radicals in $SF_6/CH_3C(O)C(O)CH_3$ mixtures and peroxy radicals in $SF_6/CH_3C(O)C(O)CH_3/O_2$ mixtures was followed. Third, the UV spectra of $CH_3C(O)C(O)CH_2\cdot$ and $CH_3C(O)C(O)CH_2O_2\cdot$ radicals were recorded.

3. Results

3.1. Relative Rate Measurements for the Reactions of Cl and F Atoms with $CH_3C(O)C(O)CH_3$ and the Reaction of F with $CH_3C(O)F$. Relative rate experiments were performed using the FTIR system at Ford Motor Company to investigate the kinetics of reactions 1, 2, and 7. The technique used is described in detail elsewhere.[11] Photolysis of molecular halogen was used as a source of halogen atoms.

$$Cl_2 \text{ (or } F_2) + h\nu \rightarrow 2 \text{ Cl (or 2 F)} \quad (3)$$

$$Cl + CH_3C(O)C(O)CH_3 \rightarrow \text{products} \quad (1)$$

$$F + CH_3C(O)C(O)CH_3 \rightarrow \text{products} \quad (2)$$

$$F + CH_3C(O)F \rightarrow \cdot CH_2C(O)F + HF \quad (7)$$

The kinetics of reaction 1 were measured relative to reactions 8 and 9. Reaction 2 was measured relative to reactions 5 and 10. Reaction 7 was measured relative to reaction 11.

$$Cl + CH_3Cl \rightarrow \text{products} \quad (8)$$

$$Cl + CH_4 \rightarrow \text{products} \quad (9)$$

$$F + CH_4 \rightarrow \text{products} \quad (5)$$

$$F + CD_4 \rightarrow \text{products} \quad (10)$$

$$F + CH_3CHF_2 \rightarrow \text{products} \quad (11)$$

Initial concentrations for the relative rate experiments were (i) 10−20 mTorr of $CH_3C(O)C(O)CH_3$, either 15 mTorr of CH_4 or 30−70 mTorr of CH_3Cl and 0.2 Torr of Cl_2 in 10−700 Torr of either O_2 or N_2 diluent, (ii) 9 mTorr of $CH_3C(O)C(O)CH_3$, 19 mTorr of the references (CH_4 or CD_4), and 1 Torr of F_2 in 700 Torr of air diluent, and (iii) 44 mTorr of $CH_3C(O)F$, 31 mTorr of CH_3CHF_2, and 1 Torr of F_2 in 700 Torr of air.

The observed loss of $CH_3C(O)C(O)CH_3$ versus those of reference compounds in the presence of either Cl or F atoms is shown in Figures 1 and 2, respectively. The loss of $CH_3C(O)F$

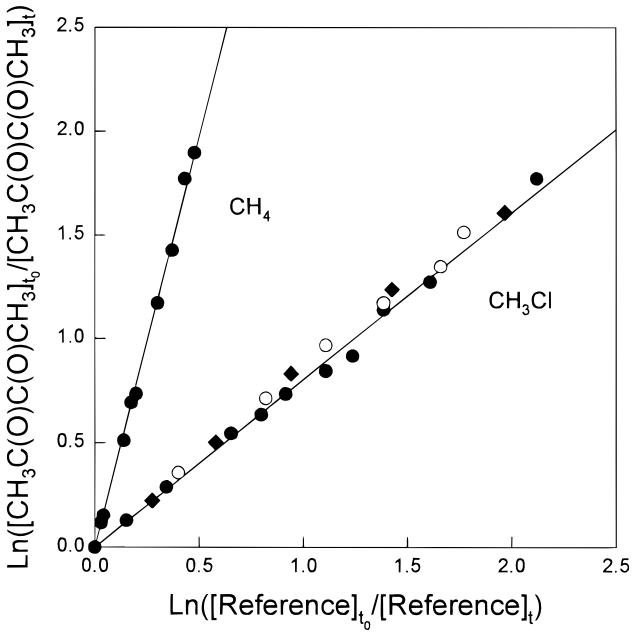

Figure 1. Loss of $CH_3C(O)C(O)CH_3$ versus CH_4 and CH_3Cl in the presence of Cl atoms: (●) 700 Torr of N_2 diluent, (○) 700 Torr of O_2 diluent, (◆) 10 Torr of N_2 diluent.

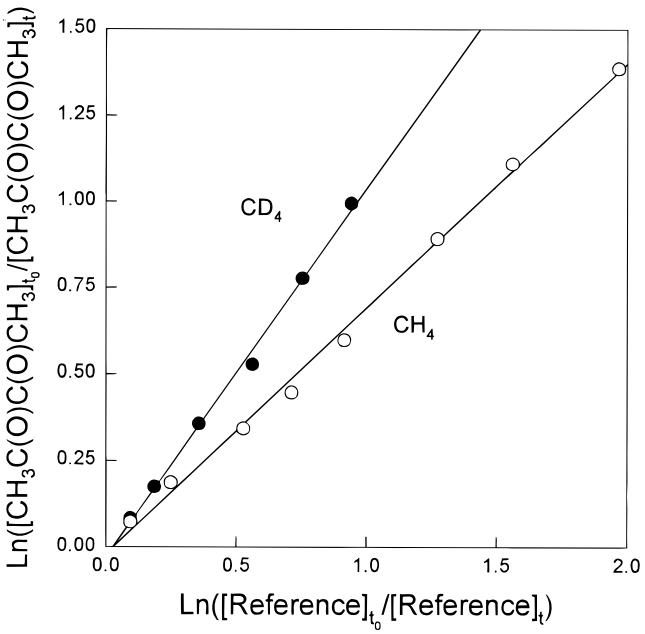

Figure 2. Loss of $CH_3C(O)C(O)CH_3$ versus CD_4 and CH_4 in the presence of F atoms in 700 Torr of air diluent.

versus CH_3CHF_2 in the presence of F atoms is shown in Figure 3. As seen from Figure 1, a reduction in total pressure from 700 to 10 Torr had no impact on k_1/k_8. It is also seen that the kinetics of reaction 1 were not impacted by the presence of oxygen. Linear least-squares analysis of the data in Figures 1, 2, and 3 gives $k_1/k_8 = 0.83 \pm 0.06$, $k_1/k_9 = 4.0 \pm 0.2$, $k_2/k_5 = 0.71 \pm 0.03$, $k_2/k_{10} = 1.06 \pm 0.07$, and $k_7/k_{11} = 0.212 \pm 0.011$. Using $k_8 = 4.8 \times 10^{-13}$,[12] $k_9 = 1.0 \times 10^{-13}$,[12] $k_5 = 6.8 \times 10^{-11}$,[13] $k_{10} = 4.7 \times 10^{-11}$,[13] and $k_{11} = 1.7 \times 10^{-11}$,[13] the five ratios give $k_1 = (4.0 \pm 0.3) \times 10^{-13}$, $k_1 = (4.0 \pm 0.2) \times 10^{-13}$, $k_2 = (4.8 \pm 0.2) \times 10^{-11}$, $k_2 = (5.0 \pm 0.3) \times 10^{-11}$, and $k_7 = (3.6 \pm 0.2) \times 10^{-12}$ cm^3 molecule^{-1} s^{-1}, respectively. We estimate that potential systematic errors associated with uncertainties in the reference rate constants add 10% uncertainty ranges for k_1, k_2, and k_7. Propagating these uncertainties gives

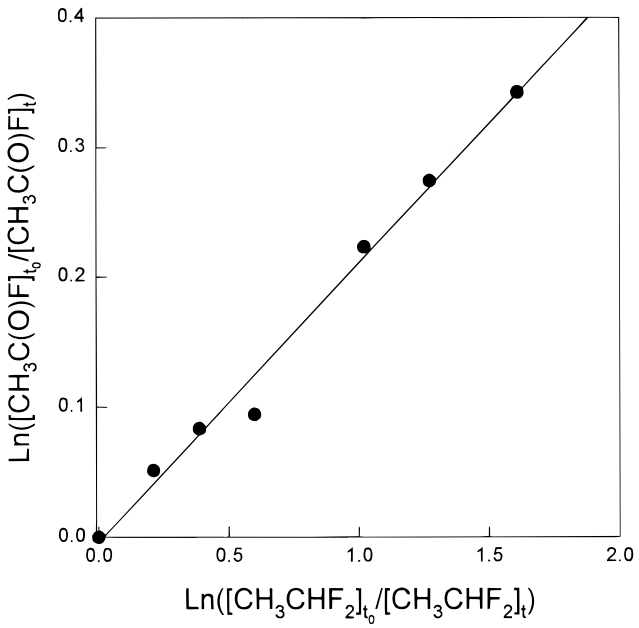

Figure 3. Loss of $CH_3C(O)F$ versus CH_3CHF_2 in the presence of F atoms in 700 Torr of air diluent.

$k_1 = (4.0 \pm 0.5) \times 10^{-13}$, $k_1 = (4.0 \pm 0.4) \times 10^{-13}$, $k_2 = (4.8 \pm 0.5) \times 10^{-11}$, $k_2 = (5.0 \pm 0.6) \times 10^{-11}$, and $k_7 = (3.6 \pm 0.4) \times 10^{-12}$ cm^3 molecule^{-1} s^{-1}. We choose to quote final values of k_1 and k_2 which are averages of those determined using the two different reference compounds together with error limits which encompass the extremes of the individual determinations. Hence, $k_1 = (4.0 \pm 0.5) \times 10^{-13}$, $k_2 = (4.9 \pm 0.7) \times 10^{-11}$, and $k_7 = (3.6 \pm 0.4) \times 10^{-12}$ cm^3 molecule^{-1} s^{-1}. Quoted errors reflect the accuracy of our measurements. The value of k_2 determined using the FTIR technique is in good agreement with that of $k_2 = (4.6 \pm 0.8) \times 10^{-11}$ cm^3 molecule^{-1} s^{-1} using the pulse radiolysis technique (see Section 3.4).

The kinetics of reaction 1 have been studied previously by Olsson et al.,[14] who report $(7.62 \pm 1.66) \times 10^{-13}$ cm^3 molecule^{-1} s^{-1}; a factor of 1.9 times greater than our result. Olsson et al. used a relative method, which required measurement of the absolute concentrations of both 2,3-butadione and the reference compound, $ClONO_2$. As discussed elsewhere,[15] we believe this method is not as robust as that employed herein where no knowledge of absolute concentrations is required and multiple reference compounds are used. No literature data is available for k_2 and k_7 to compare with our results.

3.2. Reaction Mechanism of Cl and F with 2,3-Butadione. During the product study of the Cl atom initiated oxidation of 2,3-butadione, it became apparent that reaction 1 proceeds via an unusual mechanism. In all experiments a significant yield of $CH_3C(O)Cl$ was observed. Figure 4 shows the formation of $CH_3C(O)Cl$ versus loss of $CH_3C(O)C(O)CH_3$ following UV irradiation of mixtures of 14−20 mTorr of 2,3-butadione and 0.1−0.4 Torr of Cl_2 in 700 Torr of O_2 diluent. As with all product studies, close attention needs to be paid to possible complications caused by secondary reactions in the system. To test for heterogeneous and photolytic loss of $CH_3C(O)C(O)CH_3$ and $CH_3C(O)Cl$, these compounds were introduced into the chamber and subjected to UV irradiation for 20 min; there was no discernible loss (<2%) of either compound. To test for reaction between molecular chlorine and $CH_3C(O)C(O)CH_3$, reaction mixtures were prepared and left to stand in the dark in the chamber for 20 min; there was no discernible loss (<2%) of $CH_3C(O)C(O)CH_3$. The reaction of Cl atoms with

$CH_3C(O)Cl$ proceeds with a rate constant $< 10^{-14}$ cm^3 $molecule^{-1}$ s^{-1} [16] and is not important in the present work. Four channels are possible for reaction 1:

$$Cl + CH_3C(O)C(O)CH_3 \rightarrow HCl + CH_3C(O)C(O)CH_2\cdot \quad (1a)$$

$$Cl + CH_3C(O)C(O)CH_3 \rightarrow CH_3C(O)Cl + CH_3C(O)\cdot \quad (1b)$$

$$Cl + CH_3C(O)C(O)CH_3 \rightarrow CH_3C(O)C(O)Cl + CH_3\cdot \quad (1c)$$

$$Cl + CH_3C(O)C(O)CH_3 \rightarrow CH_3Cl + CH_3C(O)C(O)\cdot \quad (1d)$$

The molar yield of $CH_3C(O)Cl$ was 0.23 ± 0.02 in O_2 diluent (see Figure 4). In the absence of O_2 the $CH_3C(O)\cdot$ radicals formed in channel 1b will react with Cl_2 to give additional $CH_3C(O)Cl$:

$$CH_3C(O)\cdot + Cl_2 \rightarrow CH_3C(O)Cl + Cl \quad (12)$$

Experiments conducted in 700 Torr of N_2 diluent gave $CH_3C(O)Cl$ yields, which were significantly greater than those in O_2 and were consistent with the formation of $CH_3C(O)\cdot$ radicals in channel 1b. There was no detectable CH_3Cl showing that channels 1c and 1d are not significant. Based upon the data given in Figure 4, it seems reasonable to conclude that reaction 1 proceeds via two channels with $k_{1a}/k_1 = 0.77 \pm 0.02$ and $k_{1b}/k_1 = 0.23 \pm 0.02$. To support the experimental evidence of channel 1b, we note that this channel is exothermic and is likely to be spontaneous at room temperature. The enthalpy of reaction 1b is -61 kJ/mol.[17]

Similar experiments were performed to investigate the mechanism of the reaction of F atoms with 2,3-butadione. Again, there are four possible channels for reaction 2:

$$F + CH_3C(O)C(O)CH_3 \rightarrow HF + CH_3C(O)C(O)CH_2\cdot \quad (2a)$$

$$F + CH_3C(O)C(O)CH_3 \rightarrow CH_3C(O)F + CH_3C(O)\cdot \quad (2b)$$

$$F + CH_3C(O)C(O)CH_3 \rightarrow CH_3C(O)C(O)F + CH_3\cdot \quad (2c)$$

$$F + CH_3C(O)C(O)CH_3 \rightarrow CH_3F + CH_3C(O)C(O)\cdot \quad (2d)$$

Figure 5 shows the formation of $CH_3C(O)F$ versus loss of $CH_3C(O)C(O)CH_3$ following UV irradiation of mixtures of 5−16 mTorr of $CH_3C(O)C(O)CH_3$ and 0.1−1 Torr of F_2 in 700 Torr of O_2, air, or N_2 diluent. The molar yield of $CH_3C(O)F$ was 0.53 ± 0.04 in O_2 and 1.18 ± 0.12 in N_2 diluent. There was no evidence of CH_3F formation in either N_2 or O_2 diluent, and we conclude that channels 2c and 2d are unimportant. The fact that the yield of $CH_3C(O)F$ in N_2 is twice that in O_2 suggests that channel 2b is the source of $CH_3C(O)F$. This channel is thermochemically possible, with a reaction enthalpy of -217 kJ/mol.[17]

Control experiments were performed which showed that $CH_3C(O)F$ is not lost via heterogeneous reactions or photolysis in the chamber. As shown in the previous section, $CH_3C(O)F$ is a factor of 14 times less reactive than $CH_3C(O)C(O)CH_3$ and secondary reaction of F atoms with $CH_3C(O)F$ will not be significant. When $CH_3C(O)C(O)CH_3/F_2/N_2$ mixtures, using $[F_2] = 0.1$ Torr, were introduced and allowed to stand in the dark in the chamber a slow ($\approx 6 \times 10^{-4}$ s^{-1}) but discernible loss of $CH_3C(O)C(O)CH_3$ was observed. In contrast, there were no observable changes when $CH_3C(O)C(O)CH_3/F_2/O_2$ mixtures were left in the chamber. It is possible that some fraction of the 2,3-butadione loss observed when $CH_3C(O)C(O)CH_3/F_2$ mixtures were left to stand in N_2 is due to reaction with F atoms present in thermal equilibrium with F_2. Using the equilibrium constant $K = [F]^2/[F_2] = 2 \times 10^{-22}$ atm,[18] it can be calculated that in the presence of $[F_2] = 0.1$ Torr the equilibrium concentrations of F atoms is 4×10^6 cm^{-3} which would lead to a 2,3-butadione loss rate of 2×10^{-4} s^{-1}; a factor of 3 less than that observed. The rate of $CH_3C(O)C(O)CH_3$ loss when $CH_3C(O)C(O)CH_3/F_2/N_2$ mixtures were subjected to UV irradiation was ≈50 times greater than the loss rate observed in

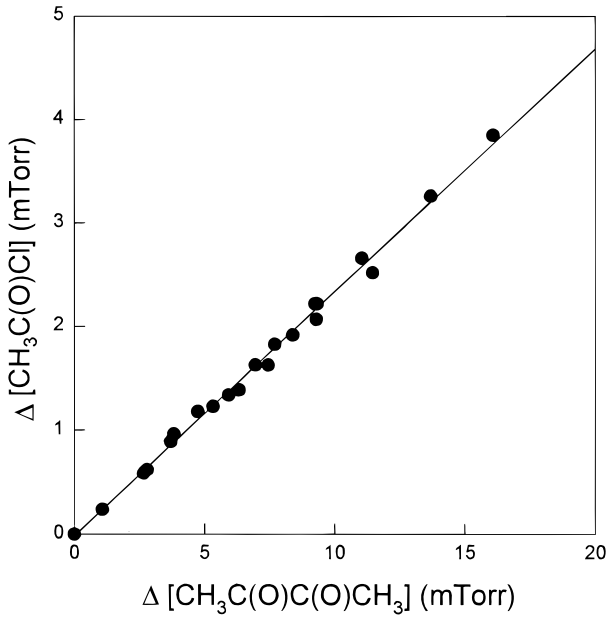

Figure 4. Formation of $CH_3C(O)Cl$ versus loss of $CH_3C(O)C(O)CH_3$ following UV irradiation of mixtures of 14−20 mTorr of $CH_3C(O)C(O)CH_3$ and 0.1−0.4 Torr of Cl_2 in 700 Torr O_2.

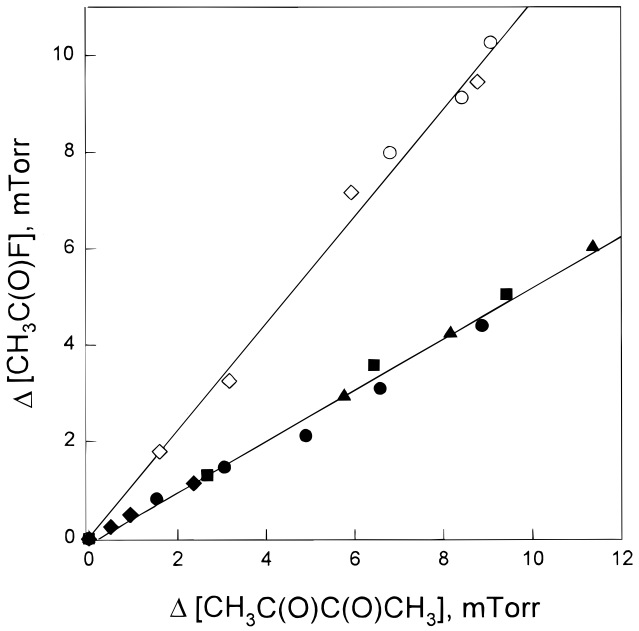

Figure 5. Formation of $CH_3C(O)F$ versus loss of $CH_3C(O)C(O)CH_3$ at a total pressure of 700 Torr: (●) UV irradiation of 15 mTorr of $CH_3C(O)C(O)CH_3$, 0.3 Torr of F_2 in 700 Torr of air diluent; (■) UV irradiation of 16 mTorr of $CH_3C(O)C(O)CH_3$, 1 Torr of F_2 in 700 Torr of O_2 diluent: (▲) UV irradiation of 16 mTorr of $CH_3C(O)C(O)CH_3$, 1 Torr of F_2 in 700 Torr of air diluent; (◆) UV irradiation of 5.5 mTorr of $CH_3C(O)C(O)CH_3$, 0.1 Torr of F_2 in 700 Torr of air diluent; (◇) dark chemistry of 11 mTorr of $CH_3C(O)C(O)CH_3$, 0.09 Torr of F_2 in 700 Torr of N_2 diluent; (○) UV irradiation of 8 mTorr of $CH_3C(O)C(O)CH_3$, 0.09 Torr of F_2 in 700 Torr of N_2 diluent.

the "dark" reaction. The observed yield of $CH_3C(O)F$ from the dark reaction was indistinguishable from that observed when the mixtures were irradiated with UV light (see Figure 5). The simplest explanation of these experimental observations is that there is a slow reaction of molecular fluorine with $CH_3C(O)C(O)CH_3$, which produces radical species. In N_2 diluent these radicals react with F_2 to give F atoms, which participate in chain reactions depleting the $CH_3C(O)C(O)CH_3$. In O_2 diluent the radicals are scavenged and chain reactions are not possible. From the viewpoint of establishing the mechanism of reaction 2, the important point is that the "dark chemistry" proceeds very slowly compared to that observed when the UV lamps are turned on and so the dark chemistry is not a significant complication.

The data obtained in N_2 in Figure 5 give $k_{2b}/k_2 = 0.59 \pm 0.06$, while that in the presence of O_2 give $k_{2b}/k_2 = 0.53 \pm 0.04$. We choose to quote a final value of k_{2b}/k_2 which is the average of these values with error limits which encompass the extremes of the individual determinations. Hence, $k_{2a}/k_2 = 0.44 \pm 0.09$, and $k_{2b}/k_2 = 0.56 \pm 0.09$.

3.3. Study of the Atmospheric Fate of $CH_3C(O)C(O)CH_2O\cdot$ Radicals. To determine the atmospheric fate of the alkoxy radical $CH_3C(O)C(O)CH_2O\cdot$ formed in reaction 14a, experiments were performed in which $CH_3C(O)C(O)CH_3$/NO/Cl_2/O_2 mixtures in 700 Torr total pressure of N_2 diluent were irradiated in the FTIR−smog chamber system:

$$Cl + CH_3C(O)C(O)CH_3 \rightarrow HCl + CH_3C(O)C(O)CH_2\cdot \quad (1a)$$

$$Cl + CH_3C(O)C(O)CH_3 \rightarrow CH_3C(O)Cl + CH_3C(O)\cdot \quad (1b)$$

$$CH_3C(O)C(O)CH_2\cdot + O_2 + M \rightarrow CH_3C(O)C(O)CH_2O_2\cdot + M \quad (13)$$

$$CH_3C(O)C(O)CH_2O_2\cdot + NO \rightarrow CH_3C(O)C(O)CH_2O\cdot + NO_2 \quad (14a)$$

$$CH_3C(O)C(O)CH_2O_2\cdot + NO \rightarrow CH_3C(O)C(O)CH_2ONO_2 \quad (14b)$$

$CH_3C(O)C(O)CH_2O\cdot$ radicals formed in reaction 14a will either decompose or react with O_2, the aim of the experiments discussed in this section was to establish the relative importance of reactions 15 and 16.

$$CH_3C(O)C(O)CH_2O\cdot + M \rightarrow CH_3C(O)C(O)\cdot + HCHO + M \quad (15)$$

$$CH_3C(O)C(O)CH_2O\cdot + O_2 \rightarrow CH_3C(O)C(O)CHO + HO_2 \quad (16)$$

It has been established previously[19] that the $CH_3C(O)C(O)\cdot$ radical formed in reaction 15 decomposes rapidly to give CO and $CH_3C(O)\cdot$ radicals and in the presence of NO_x the $CH_3C(O)\cdot$ radicals are converted into HCHO, CO_2, and $CH_3C(O)O_2NO_2$. Hence, if reaction 15 is the fate of $CH_3C(O)C(O)CH_2O\cdot$ radicals we expect to observe HCHO, CO, and CO_2, while if reaction 16 is important we expect to observe $CH_3C(O)C(O)CHO$. Based upon the reactivity of Cl atoms toward CH_3CHO and $CH_3C(O)CHO$,[19,20] it is expected that Cl atoms will react with $CH_3C(O)C(O)CHO$ with a rate constant of the order of 5×10^{-11} cm^3 molecule^{-1} s^{-1}, i.e., 100 times faster than with 2,3-butadione. To reduce complications associated with the secondary reaction of Cl atoms with $CH_3C(O)C(O)CHO$, experiments were performed with high concentrations (210−280 mTorr), and low conversions (0.1−0.8%), of 2,3-butadione. Following the UV irradiation of mixtures of 210−280 mTorr of $CH_3C(O)C(O)CH_3$, 593−599 Torr of O_2, 33 mTorr of Cl_2, and 12−23 mTorr of NO the only observed products were HCHO, CO, and CO_2. There were no features which could be attributed to $CH_3C(O)C(O)CHO$. The observed products suggest that even in the presence of 600 Torr of O_2 the dominant fate of $CH_3C(O)C(O)CH_2O\cdot$ radicals is decomposition via reaction 15. It could be argued that secondary loss of $CH_3C(O)C(O)CHO$ is more important than anticipated and that the observed HCHO, CO, and CO_2 products arise from oxidation of $CH_3C(O)C(O)CHO$. However, such oxidation would give at least two molecules of CO for each HCHO. Figure 6 shows a plot of the observed HCHO, and CO versus the combined yield of HCHO, CO, and CO_2. As seen in Figure 6 the yield of HCHO is always greater than that of CO showing that oxidation of $CH_3C(O)C(O)CHO$ is not the source of the observed products. The curvature of the HCHO and CO yield plots is explained by the loss of HCHO via reaction with Cl atoms (and possibly OH radicals). We conclude that the fate of $CH_3C(O)C(O)CH_2O\cdot$ radicals is decomposition via reaction 15. This conclusion compares well with that of Jenkin et al.[21] that decomposition via elimination of HCHO is the fate of the analogous alkoxy radical $CH_3C(O)CH_2O\cdot$ derived from acetone.

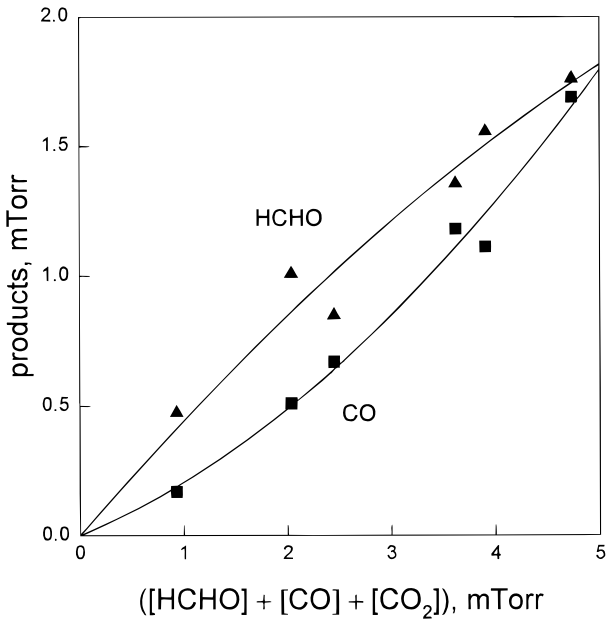

Figure 6. Observed yields of HCHO (▲) and CO (■) versus the loss of $CH_3C(O)C(O)CH_3$ (inferred from the observed yields of HCHO, CO, and CO_2) following the UV irradiation of mixtures of 210−280 mTorr of $CH_3C(O)C(O)CH_3$, 593−599 Torr of O_2, 33 mTorr of Cl_2, and 12−23 mTorr of NO. Corrections have been applied for loss of 2,3-butadione via photolysis by conducting control experiments with all reagents except Cl_2 and subtracting the small amount of HCHO and CO_2 observed. The curves are second-order regressions to aid in visual inspection of the data trends.

3.4. Absolute Rate Constant for the Reaction of F Atoms with $CH_3C(O)C(O)CH_3$. Radicals were generated by radiolysis of mixtures of 0.10−0.51 mbar of $CH_3C(O)C(O)CH_3$ and 1000 mbar of SF_6:

$$SF_6 + 2\ \text{MeV}\ e^- \rightarrow F + \text{products} \quad (4)$$

$$F + CH_3C(O)C(O)CH_3 \rightarrow \text{products} \quad (2)$$

After the radiolysis pulse a rapid increase in absorption at 250 nm was observed, followed by a slower decay. An

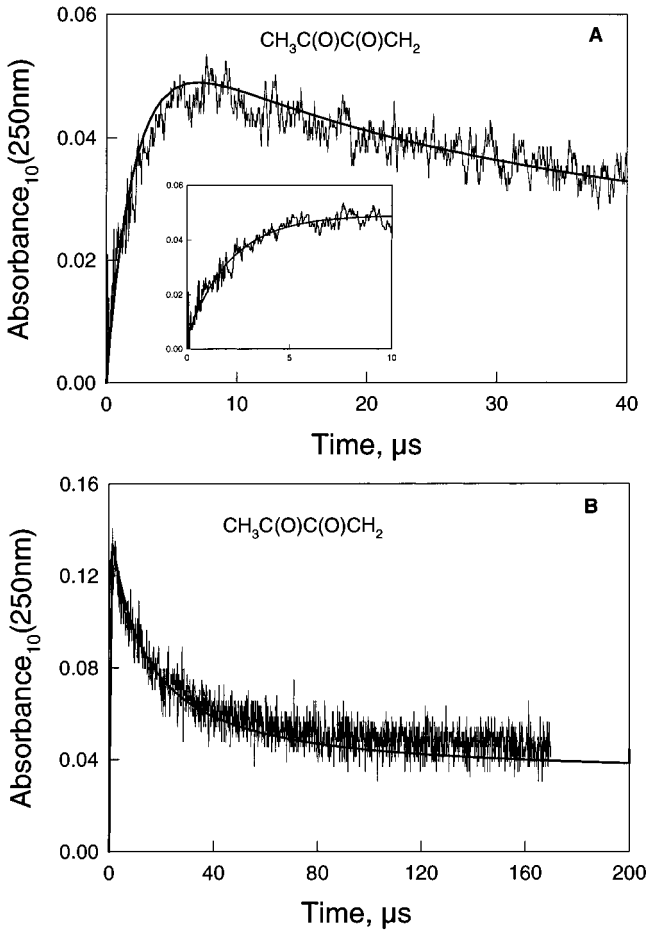

Figure 7. Absorption transients at 250 nm following pulsed radiolysis of (A) a mixture of 0.432 mbar of $CH_3C(O)C(O)CH_3$ and 1000 mbar of SF_6 at 14% of full dose, and (B) a mixture of 3 mbar of $CH_3C(O)C(O)CH_3$ and 1000 mbar of SF_6 at 32% of full dose. The smoothed lines are the simulated absorbances. The insert in panel A shows a fit of the first-order rise expression (eq I) to the initial part of the transient.

experimental transient recorded at 250 nm using 13.8% of maximum radiolysis dose and a mixture of 0.432 mbar of $CH_3C(O)C(O)CH_3$ and 1000 mbar of SF_6 is shown in Figure 7A.

An increase in transient absorption, $A(t)$, due to formation of alkyl radicals by a first-order reaction can be expressed as

$$A(t) = (A_\infty - A_o)(1 - \exp(-k^{first}t)) + A_o \qquad (I)$$

where k^{first} is the pseudo first-order formation rate constant equal to $k_2[CH_3C(O)C(O)CH_3]$. A_o and A_∞ are the absorbances at time zero, and at infinite time, respectively. A_∞ corresponds to the absorbance observed when all F atoms are converted into alkyl radicals. The three parameters A_0, A_∞, and k^{first} were varied in a nonlinear least-squares fit of eq I to the initial rise in observed transient absorption. An example of such a fit is shown in the insert in Figure 7A. The values of k^{first} obtained are plotted as a function of the initial $CH_3C(O)C(O)CH_3$ pressure in Figure 8. Linear least-squares regression gives $k_2 = (4.6 \pm 0.8) \times 10^{-11}$ which is consistent with the determination of $k_2 = (4.9 \pm 0.7) \times 10^{-11}$ cm^3 molecule^{-1} s^{-1} using the relative rate technique (see Section 3.1).

There is a small positive intercept in Figure 8 of $(8 \pm 7) \times 10^4$ s^{-1}. This intercept can be explained by the loss of radicals through radical−radical reactions such as F + R· or R· + R·, with R = $CH_3C(O)C(O)CH_2$ or $CH_3C(O)$. 2,3-Butadione was always in excess compared to alkyl radicals, and we expect that

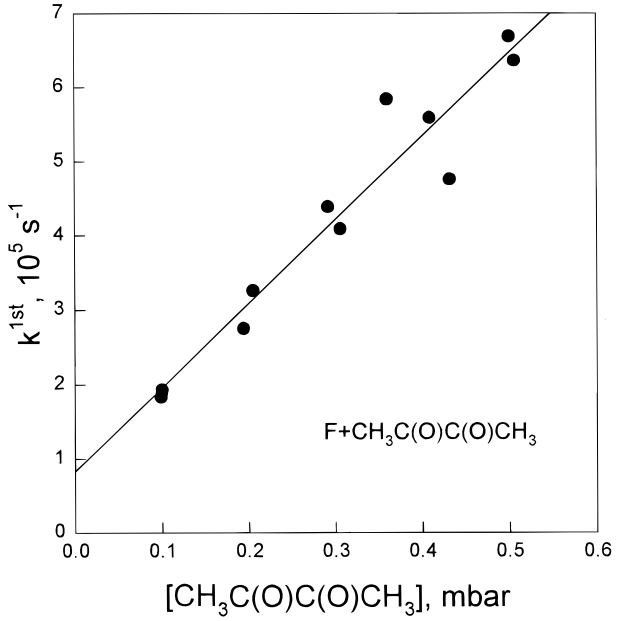

Figure 8. Plot of the pseudo first-order rate constant for the increase in absorption at 250 nm following radiolysis of $SF_6/CH_3C(O)C(O)CH_3$ mixtures versus the concentration of $CH_3C(O)C(O)CH_3$. The solid line is a linear least-squares fit.

the reactions of F atoms with R· radicals are of minor importance. The impact of R· + R· reactions is further discussed in Section 3.5, where the absorption cross section of the $CH_3C(O)C(O)CH_2$· radical is determined and the decay kinetics of the alkyl radicals is estimated. With these data and using $k_2 = 4.6 \times 10^{-11}$ cm^3 molecule^{-1} s^{-1} the absorption transients were simulated (see Figure 7A).

3.5. UV Absorption and Decay Kinetics of the $CH_3C(O)C(O)CH_2$· Radical. UV absorption spectra and the formation and decay kinetics of a large number of alkyl radicals have been studied in our laboratory using the pulse radiolysis setup.[22,23] The techniques used here are similar to those applied before.

First, to quantify the UV spectra, the formation and loss of radicals were investigated. Figure 7B shows an absorption transient at 250 nm obtained by radiolysis of a mixture of 3 mbar of $CH_3C(O)C(O)CH_3$ and 997 mbar of SF_6 using 32% of full dose. $CH_3C(O)F$ does not absorb significantly at 250 nm ($\sigma = 7 \times 10^{-21}$ cm^2 molecule^{-1} [24]) and we ascribe the rapid increase in absorption to the formation of $CH_3C(O)C(O)CH_2$· and $CH_3C(O)$· radicals and the decay to their loss via self- and cross-reactions which probably give $CH_3C(O)C(O)CH_2CH_2C(O)C(O)CH_3$, $CH_3C(O)C(O)CH_3$, and $CH_3C(O)C(O)CH_2C(O)CH_3$:

$$F + CH_3C(O)C(O)CH_3 \rightarrow HF + CH_3C(O)C(O)CH_2\cdot \quad (2a)$$

$$F + CH_3C(O)C(O)CH_3 \rightarrow CH_3C(O)F + CH_3C(O)\cdot \quad (2b)$$

$$CH_3C(O)C(O)CH_2\cdot + CH_3C(O)C(O)CH_2\cdot + M \rightarrow (CH_3C(O)C(O)CH_2)_2 + M \quad (17)$$

$$CH_3C(O)\cdot + CH_3C(O)\cdot + M \rightarrow CH_3C(O)C(O)CH_3 + M \quad (18)$$

$$CH_3C(O)\cdot + CH_3C(O)C(O)CH_2\cdot + M \rightarrow CH_3C(O)C(O)CH_2C(O)CH_3 + M \quad (19)$$

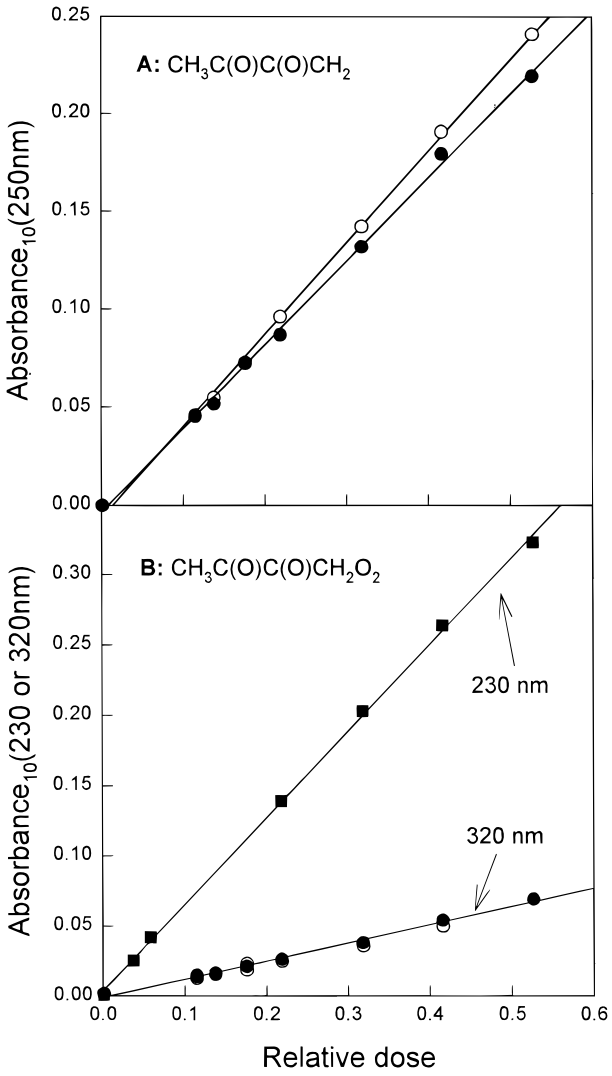

Figure 9. Maximum transient absorptions observed following radiolysis of mixtures of (A) 3 mbar of $CH_3C(O)C(O)CH_3$ and 997 mbar of SF_6, and (B) 5 mbar of $CH_3C(O)C(O)CH_3$, 50 mbar of O_2, and 945 mbar of SF_6. The transients were recorded at (A) 250 nm, and (B) 230 nm (squares) and 320 nm (circles). Filled symbols represent the maximum absorbance observed in the transient. Hollow circles represent the absorbance extrapolated to time zero using a second-order fit.

To determine the absorption cross section of the $CH_3C(O)C(O)CH_2$· radical at 250 nm it is necessary to know its concentration. F atoms that react via channel 2a are converted into $CH_3C(O)C(O)CH_2$· radicals. The observed absorbance is given by

$$\text{Absorbance} = \left(\frac{k_{2a}}{k_2}\sigma(CH_3C(O)C(O)CH_2\cdot) + \frac{k_{2b}}{k_2}\sigma(CH_3C(O)\cdot)\right)\frac{L[F]_0}{\ln 10}(\text{relative dose}) \quad \text{(II)}$$

where L is the optical path length, $L = 120$ cm, and $[F]_0$ is the F atom yield at full dose, $[F]_0 = 2.98 \times 10^{15}$ molecule cm^{-3}. The absorption cross section of $CH_3C(O)$· at 250 nm is $\sigma(CH_3C(O)\cdot) = 9 \times 10^{-19}$ cm^2 molecule^{-1}.[25] The branching ratio for reaction 2 was measured in this work, $k_{2a}/k_2 = 0.44 \pm 0.09$, and $k_{2b}/k_2 = 0.56 \pm 0.09$, see Section 3.2. The absorbance was measured at various doses and by two methods. First, the maximum absorbance was determined directly from the absorption transient. Second, the extrapolated absorbance at time zero

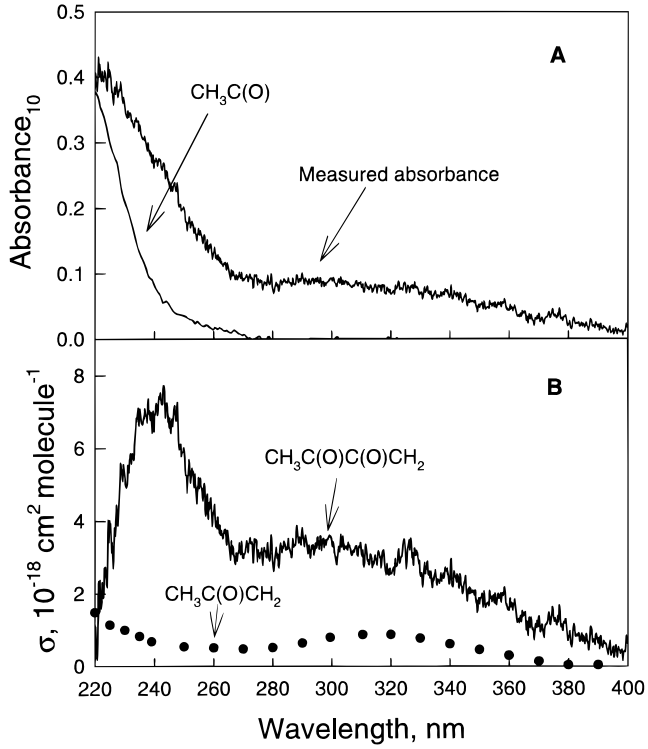

Figure 10. (A) Absorbance observed 0.6−4.6 μs after pulse radiolysis of $CH_3C(O)C(O)CH_3/SF_6$ mixtures, using 53% of maximum dose and an optical path length of 120 cm. The absorbance ascribed to $CH_3C(O)$· was calculated using the cross sections from Maricq and Szente;[25] (B) absorption spectrum of $CH_3C(O)C(O)CH_2$· (this work) and $CH_3C(O)CH_2$·.[26]

was calculated from a second-order decay fit to the absorption transients. Figure 9A shows a plot of the observed maximum absorbance (●) and the extrapolated absorbance at time zero obtained from a fit (○). As seen from Figure 9A both the observed and the extrapolated absorbance increase linearly with dose. The slopes of the straight lines through the data are 0.432 ± 0.020 and 0.465 ± 0.021. The extrapolated absorbance lies above the observed absorbance for high doses, while they tend toward equal values for low doses. This observation can be explained by the self-reaction of $CH_3C(O)C(O)CH_2$· radicals which suppresses the observed absorbance. We choose to cite the average of the two slopes with error limits which encompass the extremes of the two slopes: 0.449 ± 0.038. From this value, the absorption cross section of $CH_3C(O)C(O)CH_2$· radicals at 250 nm is determined to be $(5.4 \pm 1.0) \times 10^{-18}$ cm^2 molecule^{-1}.

The transient absorptions were simulated using a chemical mechanism consisting of reactions 2a, 2b, 17, 18, and 19. The branching ratio (Section 3.2), combined with the overall rate constant (Section 3.4) of reaction 2, gives $k_{2a} = 2.0 \times 10^{-11}$ and $k_{2b} = 2.6 \times 10^{-11}$ cm^3 molecule^{-1} s^{-1}. The kinetics of the acetyl recombination, reaction 18, have been studied by Maricq and Szente,[25] $k_{18} = 2.4 \times 10^{-11}$ cm^3 molecule^{-1} s^{-1}. k_{17} and k_{19} were varied to obtain the best fit to the measured absorption transients. A good fit was obtained using $k_{17} = k_{19} = 6 \times 10^{-11}$ cm^3 molecule^{-1} s^{-1}, but k_{17} and k_{19} are strongly correlated and we cannot determine their individual values. The transient absorbance decays to a constant level, which is ascribed to formation of products. The absorption cross section of $CH_3C(O)C(O)CH_3$ is rather small, $\sigma(CH_3C(O)C(O)CH_3) = 3 \times 10^{-20}$ cm^2 molecule^{-1}.[7] For $CH_3C(O)C(O)CH_2C(O)CH_3$ and $CH_3C(O)C(O)CH_2CH_2C(O)C(O)CH_3$ the absorbance cross sections were varied to fit the measured absorption transients, the best fit was obtained using $\sigma_{250\ nm} = 2 \times 10^{-18}$ cm^2 molecule^{-1}.

TABLE 1: Absorption Cross Sections of $CH_3C(O)C(O)CH_2\cdot$ and $CH_3(O)C(O)CH_2O_2\cdot$ Radicals

wavelength, (nm)	$\sigma(CH_3C(O)C(O)CH_2\cdot)$ $\times 10^{18}$ cm^2 molecule^{-1}	$\sigma(CH_3C(O)C(O)CH_2O_2\cdot)$ $\times 10^{18}$ cm^2 molecule^{-1}
400	0.5	0.6
395	0.5	0.7
390	0.7	0.7
385	0.8	0.8
380	1.0	0.8
375	1.3	1.0
370	1.1	0.9
365	1.3	1.0
360	1.8	1.0
355	1.9	1.2
350	1.9	1.2
345	2.2	1.4
340	2.5	1.6
335	2.4	1.7
330	2.8	1.9
325	3.2	2.1
320	2.7	2.3
315	3.0	2.7
310	3.1	3.0
305	3.3	3.3
300	3.3	3.6
295	3.3	3.7
290	3.5	3.7
285	3.3	3.7
280	3.1	3.3
275	3.2	3.0
270	3.2	2.7
265	3.4	2.4
260	4.1	2.2
255	4.9	2.3
250	5.7	2.8
245	7.0	3.5
240	7.0	4.3
235	6.7	4.9
230	5.3	5.5
225	3.2	5.6
220	0.8	3.9

Two examples of simulated transients are shown in Figure 7A,B. As seen from this figure the model gives a reasonable representation of the experimental data. Figure 7A shows that the initial rise part could be adequately simulated using the value of k_2 determined in Section 3.4.

UV absorption spectra in the range 220−400 nm were acquired using the diode array as described in Section 2.2. Figure 10A shows the measured absorption spectrum. The transient concentrations of $CH_3C(O)\cdot$ and $CH_3C(O)C(O)CH_2\cdot$ were simulated using the chemical mechanism of reactions 2a, 2b, 17, 18, and 19 described above. The mean concentrations from 0.6 to 4.6 μs of $CH_3C(O)\cdot$ and $CH_3C(O)C(O)CH_2\cdot$ were 7.4×10^{14} and 5.3×10^{14} molecule cm^{-3}, respectively. The contribution by $CH_3C(O)\cdot$ radicals to the observed absorbance was calculated using $[CH_3C(O)\cdot] = 7.4 \times 10^{14}$ molecule cm^{-3} and σ values from the literature;[25] the result is shown in Figure 10A. The UV spectrum of $CH_3C(O)C(O)CH_2\cdot$ shown in Figure 10B was obtained by subtraction of the contribution of $CH_3C(O)\cdot$ from the measured absorbance. The absorption cross section at 250 nm is consistent with the value of 5.4×10^{-18} cm^2 molecule^{-1} obtained from the dose plot. Selected absorption cross sections obtained as averages of 5 nm intervals are given in Table 1.

It is interesting to compare the UV spectrum of $CH_3C(O)C(O)CH_2\cdot$ with that of the structurally similar radical $CH_3C(O)CH_2\cdot$.[26] Both spectra have two absorption bands in the 220−400 nm region. In both cases the first band below 270 nm is the most intense and the second band has a peak maximum between 300 and 330 nm.

3.6. UV Absorption and Decay Kinetics of the $CH_3C(O)C(O)CH_2O_2$ Radical. When mixtures of 5 mbar of $CH_3C(O)C(O)CH_3$, 50 mbar of O_2, and 945 mbar of SF_6 were subjected to pulse radiolysis, transient absorbances were obtained at 230 and 320 nm. Examples of experimental absorption transients at 230 and 320 nm are shown in Figure 11A,B.

Peroxy radicals are formed from the consecutive set of reactions 2a, 2b, followed by

$$CH_3C(O)\cdot + O_2 + M \rightarrow CH_3C(O)O_2\cdot + M \quad (20)$$

$$CH_3C(O)C(O)CH_2\cdot + O_2 + M \rightarrow CH_3C(O)C(O)CH_2O_2\cdot + M \quad (13)$$

$$CH_3\cdot + O_2 + M \rightarrow CH_3O_2\cdot + M \quad (6)$$

$$2\ CH_3C(O)O_2\cdot \rightarrow 2\ CH_3C(O)O\cdot + O_2 \quad (21)$$

$$2\ CH_3C(O)C(O)CH_2O_2\cdot \rightarrow 2\ CH_3C(O)C(O)CH_2O\cdot + O_2 \quad (22)$$

$$2\ CH_3O_2\cdot \rightarrow \text{products} \quad (23)$$

$$CH_3C(O)O_2\cdot + CH_3C(O)C(O)CH_2O_2\cdot \rightarrow CH_3C(O)O\cdot + CH_3C(O)C(O)CH_2O\cdot + O_2 \quad (24)$$

$$CH_3C(O)C(O)CH_2O_2\cdot + CH_3O_2\cdot \rightarrow CH_3C(O)C(O)CH_2O\cdot + CH_3O\cdot + O_2 \quad (25)$$

$$CH_3C(O)O_2\cdot + CH_3O_2\cdot \rightarrow CH_3C(O)O\cdot + CH_3O\cdot + O_2 \quad (26a)$$

$$CH_3C(O)O_2\cdot + CH_3O_2\cdot \rightarrow \text{products} \quad (26b)$$

$$CH_3C(O)C(O)CH_2O\cdot + M \rightarrow CH_3C(O)\cdot + CO + HCHO + M \quad (27)$$

$$CH_3C(O)O\cdot + M \rightarrow CH_3\cdot + CO_2 + M \quad (28)$$

$CH_3C(O)O_2\cdot$ and $CH_3O_2\cdot$ have a negligible absorption at 320 nm,[10,27] and we attribute the rapid increase in absorption at 320 nm seen in Figure 11A to the formation of $CH_3C(O)C(O)CH_2O_2\cdot$ radicals and the decrease in absorption to loss of $CH_3C(O)C(O)CH_2O_2\cdot$ radicals via self-reaction and cross-reactions with $CH_3C(O)O_2\cdot$ and $CH_3O_2\cdot$ radicals. From the absorption transients at 230 nm it is evident that a relatively unreactive peroxy radical is formed. This is consistent with the formation of $CH_3O_2\cdot$ radicals. At 230 nm the three peroxy radicals $CH_3C(O)C(O)CH_2O_2\cdot$, $CH_3C(O)O_2\cdot$, and $CH_3O_2\cdot$ contribute to the transient absorption.

To quantify the UV absorption spectrum of the $CH_3C(O)C(O)CH_2O_2\cdot$ radical, its concentration needs to be determined. The yield of the $CH_3C(O)C(O)CH_2O_2\cdot$ radicals can be obtained only if a known fraction of the F atoms are converted into $CH_3C(O)C(O)CH_2O_2\cdot$ radicals. Unwanted secondary radical−radical reactions, such as reactions 29−33, with R = $CH_3C(O)\cdot$ or $CH_3C(O)C(O)CH_2\cdot$ must be avoided or minimized.

$$RO_2 + RO_2 \rightarrow \text{products} \quad (29)$$

$$R + R + M \rightarrow \text{products} \quad (30)$$

$$R + F \rightarrow \text{products} \quad (31)$$

$$RO_2 + R \rightarrow \text{products} \quad (32)$$

$$RO_2 + F \rightarrow \text{products} \quad (33)$$

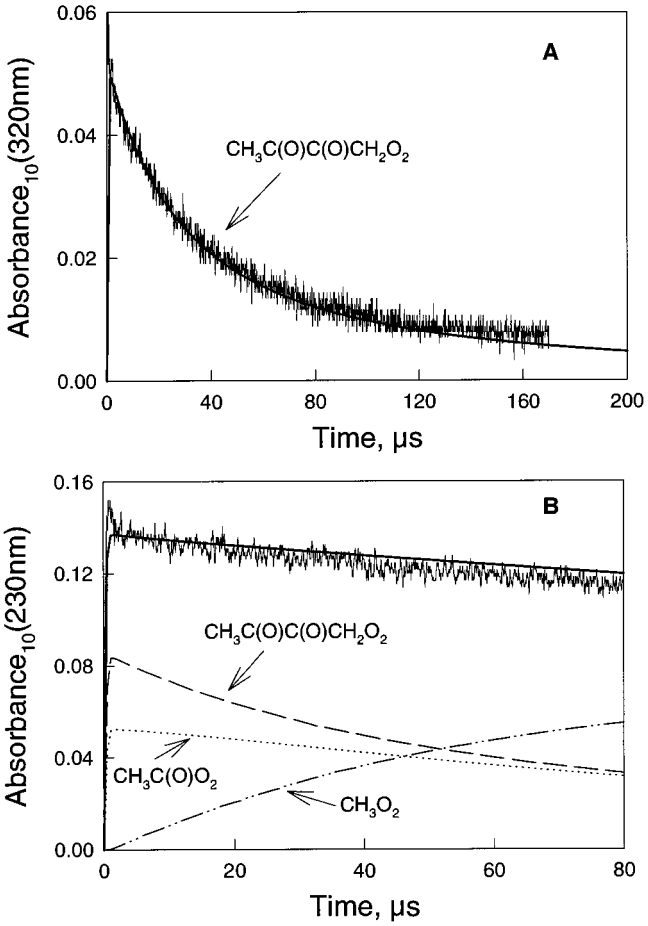

Figure 11. Absorption transients observed following radiolysis of mixtures of 5 mbar of $CH_3C(O)C(O)CH_3$, 50 mbar of O_2, and 945 mbar of SF_6 using monitoring wavelengths of (A) 320 nm and **(**B) 230 nm. Radiolysis doses were (A) 42% and (B) 22% of maximum. The smooth curves are the results of modeling the system (see text for details).

In addition, the reaction of F atoms with O_2 needs to be minimized:

$$F + O_2 + M \rightarrow FO_2 + M \qquad (34)$$

The initial concentrations of O_2 and 2,3-butadione were 50 and 5 mbar, respectively. Under these experimental conditions oxygen and 2,3-butadione were always in great excess compared to F, R, and RO_2, and reactions 30−33 are expected to be negligible. Four percent of the F atoms are converted into FO_2 ($k_{34} = 1.9 \times 10^{-13}$ [28] and $k_2 = 4.6 \times 10^{-11}$ cm^3 molecule^{-1} s^{-1}). Absolute values for the absorption cross sections of FO_2 are known[29] and were used to correct the measured UV spectrum.

The maximum absorbance at 320 nm was obtained from the absorbance transients by two methods (as discussed in Section 3.5); (1) the observed maximum absorbance was measured, and (2) the absorbance at time zero was obtained from a second-order decay fit. Figure 9B shows the observed maximum (●) and fitted transient absorption (○) as a function of the dose up to 42% of full dose. As seen from Figure 9B, the maximum and the fitted absorptions were indistinguishable and the slope of the line through the data is 0.127 ± 0.007. The absorption cross section of $CH_3C(O)C(O)CH_2O_2$• at 320 nm is obtained from the slope using the following expression

$$\text{slope} = \frac{\text{Absorbance}}{\text{(relative dose)}} = \left(0.96 \times \frac{k_{2a}}{k_2}\sigma_{320nm}(CH_3C(O)C(O)CH_2O_2\bullet)\right)\frac{L[F]_0}{\ln 10} \quad \text{(III)}$$

where $[F]_0 = (2.82 \pm 0.28) \times 10^{15}$ molecule cm^{-3} is the fluorine atom yield, at full dose and 945 mbar of SF_6. The $CH_3C(O)C(O)CH_2O_2$• yield is calculated from $k_{2a}/k_2 = 0.44 \pm 0.09$ and a 4% loss of F atom via reaction 34. $L = 120$ cm is the optical path length. At 320 nm σ ($CH_3C(O)C(O)CH_2O_2$•) = (2.0 ± 0.5) × 10^{-18} cm^2 molecule^{-1}.

The observed maximum absorbances at 230 nm plotted in Figure 9B increase linearly with radiolysis dose. The slope of a linear regression through the data is 0.616 ± 0.015. The absorption cross section of $CH_3C(O)C(O)CH_2O_2$• at 230 nm is obtained from the slope using the following expression

$$\text{slope} = \frac{\text{absorbance}}{\text{(relative dose)}} = \left(0.96 \times \frac{k_{2a}}{k_2}\sigma_{230nm}(CH_3C(O)C(O)CH_2O_2\bullet) + 0.96 \times \frac{k_{2b}}{k_2}\sigma_{230nm}(CH_3C(O)O_2\bullet) + 0.04 \times \sigma_{230nm}(FO_2)\right)\frac{L[F]_0}{\ln 10}$$

Using the literature value of $\sigma_{230\ nm}(CH_3C(O)O_2\bullet) = 2.9 \times 10^{-18}$,[27] and $\sigma_{230\ nm}(FO_2) = 4.5 \times 10^{-18}$ cm^2 molecule^{-1}[29], we obtain $\sigma_{230\ nm}(CH_3C(O)C(O)CH_2O_2\bullet) = (6 \pm 2) \times 10^{-18}$ cm^2 molecule^{-1}.

The transient absorbance of $CH_3C(O)C(O)CH_2O_2$• at 320 nm was simulated using the consecutive set of reactions 2a, 2b, and 17−19 followed by reactions 6, 13, and 20−28. The rate constants of reaction 20, 6, 21, 23, and 26 are known from the literature; $k_{20} = 5.0 \times 10^{-12}$,[30] $k_6 = 2 \times 10^{-12}$,[30] $k_{21} = 1.6 \times 10^{-11}$,[30] $k_{23} = 3.7 \times 10^{-13}$,[30] $k_{26a} = 5.5 \times 10^{-12}$, and $k_{26b} = 5.5 \times 10^{-12}$ cm^3 molecule^{-1} s^{-1}.[30] Reactions 27 and 28 are assumed to occur instantly. We are left with four unknown rate constants, k_{13}, k_{22}, k_{24}, and k_{25}. At the high oxygen concentration, reaction 13 proceeds very fast and the accuracy of k_{13} has only a minor effect on the $CH_3C(O)C(O)CH_2O_2$• yield; k_{13} was assumed equal to k_{20}. By comparison to the structurally similar acetonyl peroxy radical, $CH_3C(O)CH_2O_2$•, we expect $CH_3C(O)C(O)CH_2O_2$• to react relatively slowly with CH_3O_2•, and we assume that reaction 25 is of minor importance to the decay of $CH_3C(O)C(O)CH_2O_2$• and CH_3O_2•. In the model, k_{25} was assumed to be equal to k($CH_3C(O)CH_2O_2$• + CH_3O_2•) = 4 × 10^{-12} cm^3 molecule^{-1} s^{-1}.[31] The last two unknown rate constants, k_{22} and k_{24}, are expected to be of the same magnitude and strongly correlated. k_{24} was assumed equal to k_{21}, and k_{22} was estimated by a fit to the data at 320 nm. The best fit was obtained using $k_{22} = 2 \times 10^{-11}$ cm^3 molecule^{-1} s^{-1}. An example of a fit is shown in Figure 11A. Also, the absorption transients at 230 nm were simulated using this chemical model. The absorption cross sections of CH_3O_2• and $CH_3C(O)O_2$• at 230 nm are $\sigma_{230\ nm}(CH_3O_2\bullet) = 4.3 \times 10^{-18}$ [10] and $\sigma_{230\ nm}(CH_3C(O)O_2\bullet) = 2.9 \times 10^{-18}$ cm^2 molecule^{-1}.[27] An example of a simulated transient is shown in Figure 11B, which agrees closely with the experimentally observed transient.

The UV absorption spectrum in the range 220−400 nm was acquired using the diode array as described in Section 2.2. Figure 12A shows the measured absorbance and the calculated contributions of $CH_3C(O)O_2$•,[27] FO_2,[29] and CH_3O_2•.[10] The transient concentrations of $CH_3C(O)C(O)CH_2O_2$•, $CH_3C(O)O_2$•, FO_2•, and CH_3O_2• were simulated using the chemical

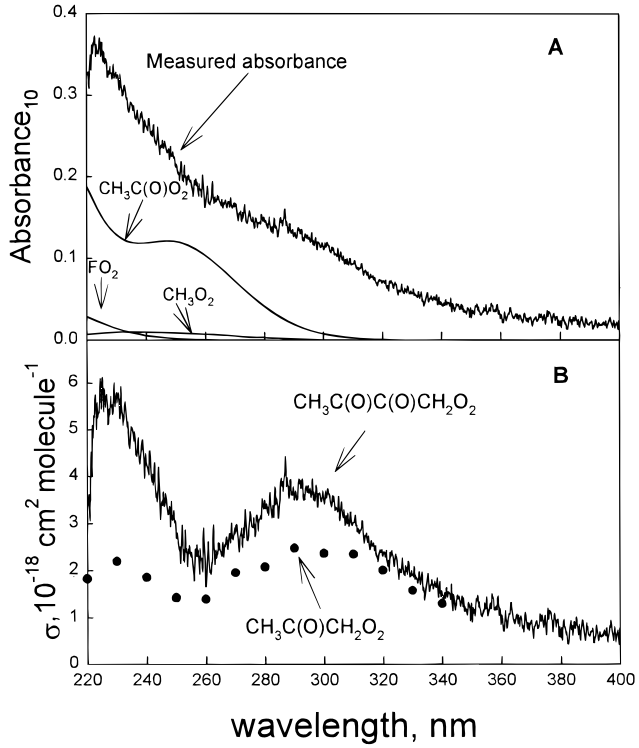

Figure 12. (A) Absorbance observed 0.6−4.6 μs after pulse radiolysis of $CH_3C(O)C(O)CH_3/SF_6/O_2$ mixtures, using 53% of maximum dose and an optical path length of 120 cm. Contributions from $CH_3C(O)O_2\cdot$, $FO_2\cdot$, and $CH_3O_2\cdot$ are shown (see text for details). (B) The absorption spectra of $CH_3C(O)C(O)CH_2O_2\cdot$ (this work) and $CH_3C(O)CH_2O_2\cdot$.[31]

mechanism of reactions 2a, 2b, 17−19, 6, 13, and 20−28 as described above. The mean concentrations from 0.6 to 4.6 μs of $CH_3C(O)C(O)CH_2O_2\cdot$, $CH_3C(O)O_2\cdot$, $FO_2\cdot$, and $CH_3O_2\cdot$ were 5.8×10^{14}, 7.8×10^{14}, 5.9×10^{13}, and 4.4×10^{13}, molecule cm^{-3}, respectively. The UV spectrum of $CH_3C(O)C(O)CH_2O_2\cdot$ shown in Figure 12B was obtained by subtraction of contributions by $CH_3C(O)O_2\cdot$, FO_2, and $CH_3O_2\cdot$ from the measured absorbance. The absorption cross sections at 230 and 320 nm are consistent with the values of 6×10^{-18} and 1.9×10^{-18} cm^2 $molecule^{-1}$ obtained from the dose plots. Selected absorption cross sections obtained as averages of 5 nm intervals are given in Table 1.

It is interesting to compare the UV spectrum of $CH_3C(O)C(O)CH_2O_2\cdot$ with that of the structurally similar peroxy radical $CH_3C(O)CH_2O_2\cdot$.[31] As shown in Figure 12B, both spectra have two absorption bands in the 220−400 nm region, with peak maxima at 230 and 300 nm, but the relative intensity of the two bands is different. In the $CH_3C(O)CH_2O_2\cdot$ spectrum both bands are equally intense, while the blue-shifted band is more intense in the $CH_3C(O)C(O)CH_2O_2\cdot$ spectrum.

4. Discussion

We present here a substantial body of spectroscopic, kinetic, and mechanistic data pertaining to the F and Cl atom initiated oxidation of 2,3-butadione. The ultraviolet absorption spectra of $CH_3C(O)C(O)CH_2\cdot$ and $CH_3C(O)C(O)CH_2O_2\cdot$ radicals over the wavelength range 220−400 nm are reported for the first time. The absorption cross sections of $CH_3C(O)C(O)CH_2\cdot$ and $CH_3C(O)C(O)CH_2O_2\cdot$ radicals were $(5.4 \pm 1.0) \times 10^{-18}$ at 250 nm and $(2.0 \pm 0.5) \times 10^{-18}$ cm^2 $molecule^{-1}$ at 320 nm, respectively.

The rate constant for the reaction of Cl atoms with $CH_3C(O)C(O)CH_3$ of $(4.0 \pm 0.5) \times 10^{-13}$ cm^3 $molecule^{-1}$ s^{-1} can be compared to $k(Cl + CH_3C(O)CH_3) = (2.4 \pm 0.1) \times 10^{-12}$,[32] and $k(Cl + CH_3CH_3) = (5.7 \pm 0.7) \times 10^{-11}$ cm^3 $molecule^{-1}$ s^{-1}.[12] It is clearly seen that the introduction of carbonyl groups in organic compounds significantly decreases their reactivity toward Cl atoms. The same trend is observed for the equivalent F atoms reactions: $k(F + CH_3C(O)C(O)CH_3) = (4.9 \pm 0.7) \times 10^{-11}$, $k(F + CH_3C(O)CH_3) = (1.1 \pm 0.3) \times 10^{-10}$,[13,33] and $k(F + CH_3CH_3) = (1.7 \pm 0.3) \times 10^{-10}$ cm^3 $molecule^{-1}$ s^{-1}.[34]

It is shown that a significant fraction of the reaction of Cl and F atoms with $CH_3C(O)C(O)CH_3$ proceeds via a novel mechanism in which the incoming halogen atom displaces a $CH_3C(O)$ group. In light of the well-established importance of the addition of Cl and F atoms to unsaturated double bonds in organic molecules it seems reasonable to speculate that the reaction channels 1b and 2b proceed via addition of the halogen to the C═O bond followed by elimination of the $CH_3C(O)$ group. For the case of the Cl atom reaction, the addition−elimination channel of reaction 1 proceeds with a rate constant of $0.23 \times 4.0 \times 10^{-13} = 9 \times 10^{-14}$ cm^3 $molecule^{-1}$ s^{-1}. This value is 10−1000 times lower than rate constants for reactions of Cl atoms with typical carbonyl compounds (acetone, butanone, formaldehyde, acetaldehyde, etc.). The addition−elimination channel is probably only of significance for carbonyl compounds whose C−H bonds are relatively unreactive toward Cl atoms. In the case of the F atom reaction, the addition−elimination channel has a rate constant of 3×10^{-11} cm^3 $molecule^{-1}$ s^{-1} and may make a nonnegligible contribution to the overall reaction of F atoms with many different carbonyl compounds.

Finally, we show here that the sole fate of the $CH_3C(O)C(O)CH_2O\cdot$ radical is decomposition via reaction 15. This is consistent with the observation that the analogous alkoxy radical $CH_3C(O)CH_2O\cdot$ derived from acetone also decomposes rapidly via elimination of HCHO.[21]

Acknowledgment. We thank Bill Kaiser (Ford) for helpful discussions.

References and Notes

(1) Atkinson, R.; Carter, W. P. L.; Winer, A. M. *J. Phys. Chem.* **1983,** *87*, 1605.
(2) Atkinson, R. *Chem. Rev.* **1985**, *85*, 177.
(3) Darnall, K. R.; Atkinson, R.; Pitts, J. N., Jr. *J. Phys. Chem.* **1979**, *83*, 1943.
(4) Siegl, W. O. Private communication, 1998.
(5) Siegl, W. O.; Zinbo, M.; Korniski, T. J.; Richert, J. F. O.; Chladek, E.; Peck, M. C.; Weir, J. E.; Schuetzle, D.; Jensen, T. E. SAE Paper No. 940581; Society of Automotive Engineers: Warrendale, PA 15096-0001, 1994.
(6) Siegl, W. O.; Korniski, T. J.; Richert, J. F. O.; Chladek, E.; Weir, J. E.; Jensen, T. E.; Zinbo, M. SAE Paper No. 961903; Society of Automotive Engineers: Warrendale, PA 15096-0001, 1996.
(7) Plum, C. N.; Sanhueza, E.; Atkinson, R.; Carter, W. P. L.; Pitts, J. N. *Environ. Sci. Technol.* **1983**, *17*, 479.
(8) Wallington, T. J.; Japar, S. M. *J. Atmos. Chem.* **1989**, *9*, 399.
(9) Hansen, K. B.; Wilbrandt, R.; Pagsberg, P. *Rev. Sci. Instr.* **1979,** *50*, 1532.
(10) Wallington, T. J.; Dagaut, P.; Kurylo, M. J. *Chem. Rev.* **1992**, *92*, 667.
(11) Wallington, T. J.; Hurley, M. D. *Chem. Phys. Lett.* **1992**, *189*, 437.
(12) DeMore, W. B.; Sander, S. P.; Golden, D. M.; Hampson, R. F.; Kurylo, M. J.; Howard, C. J.; Ravishankara, A. R.; Kolb, C. E.; Molina, M. J. Jet Propulsion Laboratory Publication 97-4; Pasadena, CA, 1997.
(13) Wallington, T. J.; Hurley, M. D.; Shi, J.; Maricq, M. M.; Sehested, J.; Nielsen, O. J.; Ellermann, T. *Int. J. Chem. Kinet.* **1993**, *25*, 651.
(14) Olsson, B. E. R.; Hallquist, M.; Ljungström, E.; Davidsson, J. *Int. J. Chem. Kinet.* **1997**, *29*, 195.
(15) Wallington, T. J.; Guschin, A.; Hurley, M. D. *Int. J. Chem. Kinet.* **1998**, *30*, 310.
(16) Shi, J.; Wallington, T. J.; Kaiser, E. W. *J. Phys. Chem.* **1993,** *97*, 6184.

(17) Lias, S. G.; Liebman, J. F.; Levin, R. D.; Kafafi, S. A. *NIST Standard Reference Database, Structures and Properties*, Version 2.01; Gaithersburg, MD, 1994.
(18) Stein, S. E.; Rukkers, J. M.; Brown, R. L. *NIST Standard Reference Database 25;* Gaithersburg, MD, 1991.
(19) Green, M.; Yarwood, G.; Niki, H. *Int. J. Chem. Kinet.* **1990**, *22*, 689.
(20) Wallington, T. J.; Skewes, L. M.; Siegl, W. O.; Wu, C.-H.; Japar, S. M. *Int. J. Chem. Kinet.* **1988,** *20*, 867.
(21) Jenkin, M. E.; Cox, R. A.; Emrich, M.; Moortgat, G. K. *J. Chem. Soc., Faraday Trans.* **1993**, *89*, 2983.
(22) Wallington, T. J.; Bilde, M.; Møgelberg, T. E.; Sehested, J.; Nielsen, O. J. *J. Phys. Chem*. **1996**, *100*, 5751.
(23) Wallington, T. J.; Ellermann, T.; Nielsen, O. J. *Res. Chem. Intermed.* **1994**, *20*, 265.
(24) Rattigan, O. V.; Wild, O.; Jones, R. L.; Cox, R. A. *J. Photochem. Photobiol., A* **1993**, *73*, 1.
(25) Maricq, M. M.; Szente, J. J. *Chem. Phys. Lett.* **1996**, *253*, 333.
(26) Cox, R. A.; Munk, J.; Nielsen, O. J.; Pagsberg, P.; Ratajczak, E. *Chem. Phys. Lett.* **1990**, *173*, 206.
(27) Maricq, M. M.; Szente, J. J. *J. Phys. Chem.* **1996**, *100*, 4507.
(28) Ellermann, T.; Sehested, J.; Nielsen, O. J.; Pagsberg, P.; Wallington, T. J. *Chem. Phys. Lett.* **1994**, *218*, 287.
(29) Maricq, M. M.; Szente, J. J. *J. Phys. Chem.* **1992**, *96*, 4925.
(30) Atkinson, R.; Baulch, D. L.; Cox, R. A.; Hampson, R. F.; Kerr, J. A.; Troe, J. *J. Phys. Chem. Ref. Data.* **1992**, *21*, 1125.
(31) Bridier, I.; Veyret, B.; Lesclaux, R.; Jenkin, M. E. *J. Chem. Soc., Faraday Trans.* **1993**, *89*, 2993.
(32) Wallington, T. J.; Andino, J. M.; Ball, J. C.; Japar, S. M. *J. Atmos. Chem.* **1990**, *10*, 301.
(33) Smith, D. J.; Setzer, D. W.; Kim, K. C.; Bogan, D. J. *J. Phys. Chem.* **1977**, *81*, 898.
(34) Moore, C.; Smith, I. W. M. *J. Chem. Soc., Faraday Trans.* **1995**, *91*, 3041.